Size of x-ray coherent region and nonlinear microwave response of epitaxial $YBa_2Cu_3O_{7-x}$ films

S. V. Baryshev,[1,*] E. E. Pestov,[2,†] A. V. Bobyl,[1] Yu. N. Nozdrin,[2] and V. V. Kurin[2]
[1]*Ioffe Physico-Technical Institute, Russian Academy of Sciences, 26 Polytekhnicheskaya, St.-Petersburg 194021, Russia*
[2]*Institute for Physics of Microstructures, Russian Academy of Sciences, GSP-105, Nizhny Novgorod 603950, Russia*
(Received 3 April 2007; revised manuscript received 4 July 2007; published 28 August 2007)

$YBa_2Cu_3O_{7-x}$ epitaxial films have been studied by near-field nonlinear microwave and low-temperature scanning microscopies. A correlation between the half-widths of peaks in the temperature dependences of third-harmonic power, electron-beam-induced voltage, and the size of the x-ray coherent region (average grain size) was revealed. According to a two-phase model, the nonlinear microwave response is determined by intragrain vortex pinning at large grain sizes and by pinning at intergrain boundaries at small grain sizes. The results of model calculations suggest that a threefold increase in the average grain size can result in a 100-fold decrease in the nonlinear coefficient of $YBa_2Cu_3O_{7-x}$ films.

DOI: 10.1103/PhysRevB.76.054520 PACS number(s): 74.25.Nf, 74.25.Qt, 74.78.Bz

At present, high-temperature superconducting (HTSC) films are successfully used in transmission lines, filters, and antennas.[1–3] However, the nonlinearity of the microwave response of HTSC films at high power levels gives rise to intermodulation distortions,[4,5] generation of higher harmonics of the basic frequency,[6] and higher microwave loss,[7] which restricts the applicability range of these films. As it has been shown earlier, the nonlinear effects in the HTSC films may be associated both with intrinsic sources of the nonlinearity and with the real microstructure of a sample. In particular, the nonlinear microwave response of homogeneous superconductors has been attributed to pair-breaking effect in *d*-wave[4,5,8] or *s*-wave[9] superconductors and nonlinearity of a superconductor with a mixed order parameter.[10] At the same time, mechanisms of technological origin have been suggested for explaining the nonlinear microwave properties of these films: structural defects,[9,11,12] edge effects,[13] chaotic Josephson boundaries (weak links),[7,14,15] and thermal nonlinearity.[16] However, all the characteristic current densities j_{NL} for various nonlinearity mechanisms tend to zero at temperatures close to T_c, and many mechanisms can contribute to the overall nonlinear response. Therefore, the nature of the nonlinear microwave response in the vicinity of T_c remains unclear despite the large number of theoretical and experimental studies devoted to this issue.

Modern microwave superconductor electronics uses sufficiently thick (0.5–1 μm) $YBa_2Cu_3O_{7-x}$ films. Therefore, the influence exerted by the microscopic structure of such $YBa_2Cu_3O_{7-x}$ films on their nonlinear microwave properties and electrical parameters was examined in this study. A correlation between the size of the x-ray coherent region (average grain size) and half-widths of peaks in the temperature dependences of the third-harmonic (TH) power and electron-beam-induced voltage (EBIV) signal at temperatures close to T_c was revealed. It was shown in terms of the effective-medium model that the nonlinear microwave response is due to (i) intragrain vortex pinning at large grain sizes and (ii) pinning at intergrain boundaries at small grain sizes.

Epitaxial $YBa_2Cu_3O_{7-x}$ films of thickness $d=0.7$–0.9 μm were produced by magnetron sputtering from targets of compositions 1:2:3 and 2:3:5. The films were grown on $LaAlO_3$ substrates in the Ar/O gas mixture under pressure of 40 Pa at a substrate temperature of 750 °C. The temperature of the superconducting transition found by means of dc measurements was in the range of 86–92 K, with a transition region width of 0.15–3.6 K.

$YBa_2Cu_3O_{7-x}$ films had a depinning current density $j_p(77\ \mathrm{K})$ of 10^5–1.4×10^6 A/cm^2. The value of $j_p(77\ \mathrm{K})$ was determined in terms of the Bean model from the residual magnetic field B_z found by noncontact Hall probe measurements.[17] After the magnetic field was raised to $B \geqslant 600$ Oe, which provided a complete penetration of the magnetic flux into the film, and was then lowered to zero, the maximum magnitude of the captured field $B_z(x,y)$ was determined by the Hall probe. Then, the value of j_p, averaged over the film surface, was calculated using the formula[18] $j_p = c\ \max\{B_z\}/2\pi d_0 \ln(L/R_H)$ in terms of the critical-state model $j=j_p=\mathrm{const}$. Here, d_0 and L are the thickness and the linear dimension of the film; $R_H \approx 250$ μm is the parameter that describes the spatial resolution of the Hall probe.

Statistically averaged structural parameters of the films were determined by measuring x-ray diffraction curves with a RIGAKU (D_{MAX}-B/RC) diffractometer in the θ-2θ scanning mode, with a special collimation scheme aimed to reduce the beam divergence ($\lambda_{Cu}=1.541\ 83$ Å). The average size of the x-ray coherent region was calculated for each sample (0.19–0.76 μm) by processing the x-ray data with the mosaic-block model formulas.[19] In what follows, by the average grain size a we mean the average size of the x-ray coherent region. In particular, the widths of the (005) θ-2θ peak for samples with $a=660$ and 754 nm are 0.05° and 0.04°, respectively.[20,21] The epitaxial structure and high crystal quality of studied films were also proven with x-ray diffraction analysis. The full width at half maximum of the (005) rocking curves estimated by ω scan technique was less than 0.5° for all films.[20]

Two independent probing techniques were used to reveal correlations between the structural and electrical parameters. For local analysis of the nonlinear microwave response, a near-field nonlinear microwave technique was used.[17,22] This method is based on recording a TH signal using a near-field probe with inductive coupling. The probe has the form of a wire, 2 mm long and 50 μm in diameter, which connects the outer and inner conductors of a coaxial cable. A microwave

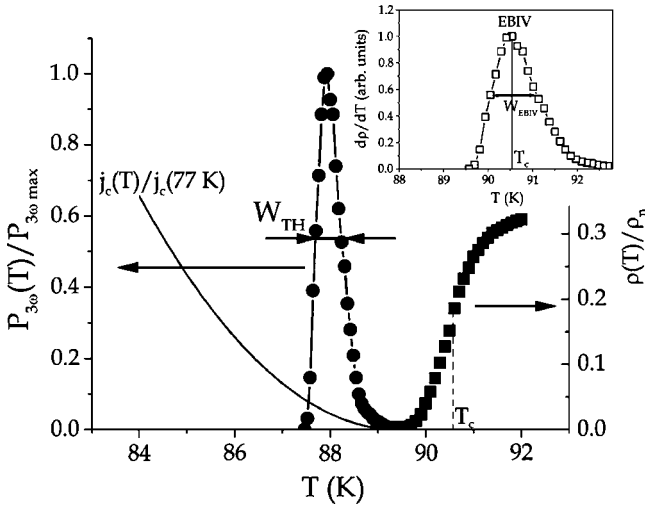

FIG. 1. Temperature dependences of the third harmonic power $P_{3\omega}(T)$ normalized to maximum magnitude $P_{3\omega\,\max}$, microbridge resistivity $\rho(T)$ normalized to normal phase resistivity ρ_n (at $T=300$ K), and temperature dependence of effective critical current $j_c(T)$ normalized to $j_c(77\ \mathrm{K})=5\times10^6\ \mathrm{A/cm^2}$ for $YBa_2Cu_3O_{7-x}$ film with $a=470$ nm. The inset represents the temperature dependence of EBIV signal curve normalized to its maximum magnitude. The figure also shows the critical temperature of superconductor transition T_c defined with EBIV technique. The main parameters used in the paper are pointed out: half-widths of peaks in the temperature dependences of third-harmonic power, W_{TH}, and EBIV signal, W_{EBIV}.

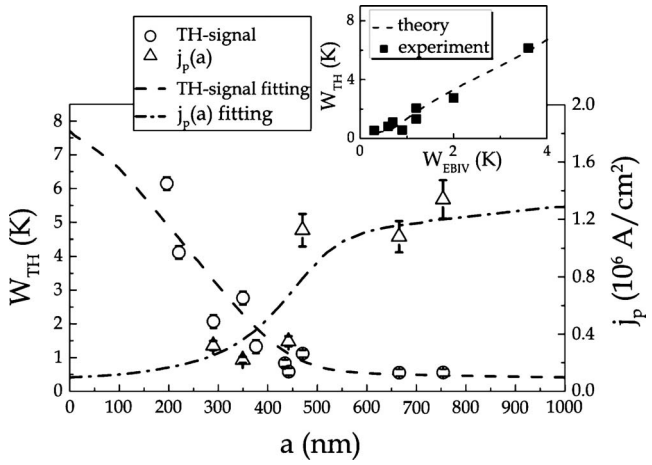

FIG. 2. Half-widths of the TH signal W_{TH} (open circles) and the pinning current j_p (open triangles) vs the average grain size for $YBa_2Cu_3O_{7-x}$. The dashed lines are fitting curves for $W(a)$ and $j_p(a)$, calculated in terms of the effective-medium model for the nonlinear response, EBIV signal, and pinning current. Inset: the experimental and theoretical correlation functions between W_{TH} and W_{EBIV} parameters obtained at the same grain sizes. Both the MW response and EBIV signals were measured in the 77–95 K range and the pinning current at 77 K.

signal with a basic frequency $\nu=472$ MHz is nearly totally reflected because the probe impedance is considerably lower than the wave impedance of the coaxial cable. This gives rise to a high density current in the wire, which induces a rather strong quasistatic magnetic field localized on a scale of the order of the probe diameter. Higher harmonics are generated because of the nonlinear properties of a superconducting film and are picked up by the same probe. The incident power at the first-harmonic frequency was 100 mW. The half-width W_{TH} (Fig. 1) of the peak in the temperature dependence of the TH power $P_{3\omega}(T)$ at temperatures close to T_c was determined using this near-field technique and the function $W_{TH}(a)$ was plotted (Fig. 2, open circles).

The second procedure, low-temperature scanning electron microscopy[23,24] (LTSEM) is based on thermal heating by an electron beam of a local area of a superconducting microbridge, which changes its local resistivity ρ and the voltage recorded. This EBIV signal is proportional to the temperature derivative of the local resistivity of this area (Fig. 1). This procedure makes it possible both to determine the temperature dependence of the local resistivity $\rho_i(T)$ from the $f(T_{ci})$ function, the EBIV-signal curve of single film fragment, and to plot the distribution function of film fragments over critical temperatures, $F(T_{ci})$. The fragment size of about 4 μm is defined by the sizes of the probe and heated region. In the case of LTSEM, a convolution procedure was performed for the $F(T_{ci})$, $f(T_{ci})$ functions for determining the half-width, because the temperature dependence of the integral resistivity may differ from that of local area resistivities. First, the temperature dependence of the local resistivity of fragments, $\rho_i(T)$, was calculated from the curve of the EBIV signal of a fragment, $f(T_{ci})$.[24,25] Then, the resistivity $\langle\rho\rangle(T)$ on a scale of the order of the microwave probe size was found in the effective-medium approximation for the two-dimensional case.[25,26] Finally, the reconstructed function $S_{EBIV}(T)$ was found from the temperature dependence $\langle\rho\rangle(T)$ on the same scale. The inset in Fig. 2 shows the half-width of the function $S_{EBIV}(T)$, $W_{EBIV}(a)$. For EBIV measurements, $100\times500\ \mu\mathrm{m}^2$ microbridges with contact pads were fabricated by ion etching from $YBa_2Cu_3O_{7-x}$ films studied by near-field microwave technique. The EBIV signals were measured with a CamScan Series 4-88 DV 100 electron microscope equipped with a nitrogen cooling system, ITC temperature control unit, and an intrachamber preamplifier for reducing the noise intensity. The standard four-probe measuring scheme was used. Both the microwave (MW) response and EBIV signals were measured in the 77–95 K range.

It can be seen from Fig. 2 that the half-widths of the signals, obtained by two independent techniques, decrease as the average grain size increases. The inset in Fig. 2 shows the correlation function between W_{TH} and W_{EBIV}, which demonstrates a fundamental relationship between these parameters.

In order to elucidate the physical mechanism by which the microstructure affects the electrical and microwave parameters of HTSC films (Fig. 2), let us consider a phenomenological model of a two-phase superconductor: a film that consists of cylindrical superconducting grains embedded in a host medium (matrix). It is assumed in this approach that the physical properties of the grains and the matrix are the same for all of the films studied, and samples differ from each other only in the relative volume fractions of these phases.

Thus, the first phase describes the superconducting properties of a grain, and the second one represents the grain boundaries in a superconducting film. In particular, this approach also allows modeling of superconducting grains connected by Josephson junctions (weak links).[7,15]

Let us find the current-voltage (I-V) characteristic $\langle E\rangle(\langle j\rangle)$ of a two-phase medium containing a phase of cylindrical inclusions (grains) of radius a and volume fraction $p=V_1/V$ (where V_1 is the total volume of all grains and V the volume of the superconductor as a whole). For calculations, we use the effective-medium approximation[25,26] which is valid at any volume fractions p of inclusions:

$$p\frac{\langle\rho\rangle-\rho_1(j_1,T)}{\langle\rho\rangle+\rho_1(j_1,T)}+(1-p)\frac{\langle\rho\rangle-\rho_2(j_2,T)}{\langle\rho\rangle+\rho_2(j_2,T)}=0, \tag{1}$$

where $\langle\rho\rangle=\langle E\rangle/\langle j\rangle$ is the effective resistivity of the superconductor, and $\rho_1=E_1(j_1,T)/j_1$ and $\rho_2=E_2(j_2,T)/j_2$ are the resistivities of the first and second media, respectively. We use the phenomenological approach for describing the main specific features of the I-V characteristic of these superconductors and take as a model dependence the I-V characteristic of a nonhysteretic Josephson junction.[27] In this case, the electric field strengths $\vec{E}_{1,2}$ are related to the current densities in both media, $\vec{j}_{1,2}$, by

$$\vec{E}_{1,2}(j_{1,2},T)=\rho_{n1,2}\,\mathrm{sgn}(j_{1,2})\sqrt{j_{1,2}^2-j_{c1,2}^2(T)}\frac{\vec{j}_{1,2}}{j_{1,2}}, \tag{2}$$

where $j_{c1}(T)$ and $j_{c2}(T)$ and ρ_{n1} and ρ_{n2} are the critical current densities and resistivities of these phases, respectively. Further, we assume that the effective current density $\langle j\rangle$ in the superconductor is given by

$$\langle j\rangle=pj_1+(1-p)j_2, \tag{3}$$

where j_1 and j_2 are the current densities in the grains and matrix, respectively. Finally, taking into account the expression for the effective electric field strength $\langle E\rangle$,

$$\langle E\rangle=pE_1(j_1,T)+(1-p)E_2(j_2,T), \tag{4}$$

and solving numerically the system of equations (1)–(4), we can determine $\langle E\rangle$ and the I-V characteristic of the composite two-phase superconductor, $\langle E\rangle(\langle j\rangle)$.

The results of a numerical fitting to the dependence of W_{TH} and W_{EBIV} on the average grain size a, performed in terms of the effective-medium model, are also shown in Fig. 2 and its inset (dashed lines). It was assumed that the dependence of p on the grain size is given by the following expression:[7]

$$p(a)=\left(\frac{a}{a+d}\right)^2, \tag{5}$$

where d is a phenomenological parameter characterizing the linear dimension of the intergrain medium. Experimental data on $W_{TH}(a)$, $W_{EBIV}(a)$, and $j_p(77\ \mathrm{K})(a)$ were fitted with $j_c(a)$, $W(a)$ theoretical curves with least-squares method regarding $j_{c1}(77\ \mathrm{K})$, $j_{c2}(77\ \mathrm{K})$, and d as model fitting parameters. These theoretical dependences $j_c(a)$ and $W(a)$ were found by means of I-V characteristics of two-phase medium $\langle E\rangle(\langle j\rangle)$ calculated for various grain sizes with expression (5).

It can be seen from Fig. 2 that, as the average grain size a increases and, consequently, so does the volume fraction of inclusions, $p\sim a^2$, the half-widths W_{TH} and W_{EBIV}, i.e., the width of the superconducting transition, decrease. It follows from the model calculation that such a dependence can exist if the medium consists of single crystals (grains) embedded in a superconducting matrix with a suppressed critical current $j_{c1}(T)>j_{c2}(T)$. In this case, the current starts to concentrate in grains as the volume of the single-crystal phase in the superconductor grows, and this leads to an increase in the effective current density of the superconductor, $\langle j_c\rangle$.

According to the two-phase model, an increase in $j_c(a)$ leads to a decrease in $W(a)$ as a grows. Experiments in which the depinning current density j_p was measured at various grain sizes a (Fig. 2, open triangles) also demonstrated a good qualitative and quantitative agreement with the model of a two-phase superconductor: the half-widths W_{TH} and W_{EBIV} decrease as the average grain size grows, and this occurs because of the increase in j_p. Thus, the presence of the experimental correlations between W_{TH}, W_{EBIV}, and $j_p(77\ \mathrm{K})$ suggests that the nonlinear and transport properties of $YBa_2Cu_3O_{7-x}$ films are determined by a vortex pinning. This model conclusion is proven by the presence of the pointed out experimental correlations between W_{TH}, W_{EBIV}, and $j_p(77\ \mathrm{K})$ with statistically significant correlation coefficient R ($R=0.81$, $\Delta R=0.72$).[28]

Note also that generally, the critical current in a superconductor can be determined both by a bulk pinning and the presence of edge and/or surface barrier. However, local techniques have allowed us to avoid influence of the edge effects on the measurements of the TH signal and the EBIV signal. In particular, in the near-field nonlinear microwave microscopy case, the probe was placed in the film center. It has allowed us to exclude the vortex penetration through the film edges, because the magnetic field has been localized on a scale of the order of the probe diameter of $\sim 50\ \mu$m. In the EBIV case, scanning of the sample was also made at distances at which the edge barrier did not influence on our measurements. Therefore, we think that in our case, a critical current in the epitaxial $YBa_2Cu_3O_{7-x}$ films is determined by the bulk pinning, and the edge and/or surface barrier can be neglected at measurements of the TH power and EBIV signal.

Further, since the two-phase model predicts that the superconducting properties are controlled only by the intra- or intergrain medium at $p=1$ or $p=0$, one can obtain the limiting parameters of the material, namely, the critical currents of intragrain $j_{c1}(77\ \mathrm{K})$ and intergrain $j_{c2}(77\ \mathrm{K})$ media using the theoretical dependences $j_c(a)$ and $W(a)$. To evaluate these parameters at temperatures close to T_c, linear temperature dependences of the critical currents $j_{c1,2}(T)=j_{c1,2}^0(1-T/T_c)$ were chosen because they were in agreement with the temperature dependence of $j_p(T)$ of the films studied. Thus, the critical pinning currents $j_{p1}(77\ \mathrm{K})=1.4\times10^6\ \mathrm{A/cm^2}$ for intragrain medium and $j_{p2}(77\ \mathrm{K})=10^5\ \mathrm{A/cm^2}$ for intergrain medium are well consistent with

the critical currents for both media, obtained by calculations in terms of the two-phase superconductor model: (a) TH signal, $j_{c1}(77\ \mathrm{K})=2.5\times10^6\ \mathrm{A/cm^2}$ and $j_{c2}(77\ \mathrm{K})=10^5\ \mathrm{A/cm^2}$; (b) EBIV signal, $j_{c1}(77\ \mathrm{K})=4\times10^6\ \mathrm{A/cm^2}$ and $j_{c2}(77\ \mathrm{K})=3\times10^5\ \mathrm{A/cm^2}$. Thus, the phenomenological model of the superconductor suggests that the nonlinear and transport properties of $YBa_2Cu_3O_{7-x}$ films near T_c are determined by intragrain vortex pinning at large grain sizes and by pinning at intergrain boundaries at small grain sizes.

It should also be noted that it follows from the experimental dependences (Fig. 2) that a threefold increase in the average grain size leads to a sixfold decrease in W_{EBIV} and a tenfold decrease in W_{TH} and to an order-of-magnitude rise in the critical pinning current j_p of the superconductor. It is well known that, in the weak-signal approximation, i.e., at a current density j much less than a critical current density j_c, $E(j)$ can be written as[29] $E=\alpha(T)j+\beta(T)j^3$, and the nonlinear coefficient $\beta(T)$ is inversely proportional to a squared characteristic nonlinearity current density of the superconductor j_{NL}, $\beta(T)\sim\frac{1}{j_c^2(T)}$.[7,17] In this case, a threefold increase in the average grain size leads to a 100-fold decrease in the nonlinear coefficient. Such a decrease in $\beta(T)$ results in a 10^4-fold reduction of the intermodulation level and third-harmonic power because the third-harmonic power quadratically depends on the nonlinear coefficient,[30] $P_{3\omega}\sim E_{3\omega}^2\sim\beta^2\sim j_{NL}^{-4}$. This diminishes intermodulation distortions of the signal, loss, and heating in superconducting microwave devices,[16] thereby extending the applicability range of $YBa_2Cu_3O_{7-x}$ films.

Finally, we would like to tell some words about the control method of the grain size. It is known that in the magnetron technique case, the average grain size of the epitaxial $YBa_2Cu_3O_{7-x}$ films can be controlled by the film growth conditions and, primarily, by the substrate temperature and composition of targets. At various growth conditions, the average size of the x-ray coherent region may be varied in the range of $0.05-1\ \mu$m.[7,31] Therefore, the film manufacturing process allows us to obtain the film with given average grain size by means of optimization of these technological parameters. Thus, the average grain size can be used as a controllable parameter for improving of the nonlinear properties in $YBa_2Cu_3O_{7-x}$ films.

In summary, the effect of the microstructure of $YBa_2Cu_3O_{7-x}$ films on their nonlinear microwave properties and electrical parameters was studied. A correlation between the half-widths W_{TH} and W_{EBIV} and the size of the x-ray coherent region (average grain size) was experimentally revealed. At temperatures close to T_c, the contributions to the nonlinear microwave response from intragrain and intergrain vortex pinning were distinguished in the framework of the phenomenological model of a two-phase superconductor. The possibility of diminishing the nonlinear effects in $YBa_2Cu_3O_{7-x}$ films by making the average grain size larger was demonstrated.

The authors are grateful to A. A. Andronov, Yu. M Galperin, S. V. Gaponov, R. A. Suris, M. R. Trunin, O. G. Vendik, and A. A. Utkin for helpful discussions and to M. A. Yagovkina and J. N. Drozdov for performing the x-ray structural analysis of $YBa_2Cu_3O_{7-x}$ films. The study was supported by the Russian Foundation for Basic Research (Grant No. 06-02-16592), "Scientific schools" program, and ISTC 2920.

*lolapalooza@mail.ru
†pestov@ipm.sci-nnov.ru

[1] C. Collado, J. Mateu, O. Menendez, and J. M. Callaghan, IEEE Trans. Appl. Supercond. **15**, 992 (2005).
[2] Y. Tsutumi, H. Kanaya, and K. Yoshida, IEEE Trans. Appl. Supercond. **43**, 1020 (2005).
[3] J. Mateu, J. C. Booth, and B. H. Moekly, Appl. Phys. Lett. **90**, 012512 (2007).
[4] T. Dahm and D. J. Scalapino, J. Appl. Phys. **81**, 2002 (1997).
[5] M. I. Salkola and D. J. Sacalapino, Appl. Phys. Lett. **86**, 112509 (2005).
[6] C. Wiker, Z.-Y. Shen, P. Pang, W. L. Holstein, and D. W. Face, IEEE Trans. Appl. Supercond. **5**, 1665 (1995).
[7] P. P. Nguyen, D. E. Oates, G. Dresselhaus, and M. S. Dresselhaus, Phys. Rev. B **48**, 6400 (1993).
[8] T. Dahm and D. J. Scalapino, Phys. Rev. B **60**, 13125 (1999); D. Agassi and D. E. Oates, *ibid.* **72**, 014538 (2005).
[9] L. P. Gorkov and G. M. Eliashberg, Sov. Phys. JETP **27**, 328 (1968); I. Ciccarello, C. Fasio, M. Guccione, M. Li. Vigni, and M. R. Trunin, Phys. Rev. B **49**, 6280 (1994); K. Kim and D. Stroud, J. Appl. Phys. **100**, 113905 (2006).
[10] V. V. Kurin and A. A. Utkin, JETP **100**, 576 (2005).
[11] 11 C. J. van der Beek, M. Konczykowski, V. M. Vinokur, T. W. Li, P. H. Kes, and G. W. Crabtree, Phys. Rev. Lett. **74**, 1214 (1995).
[12] A. P. Zhuravel, S. M. Anlage, and A. V. Ustinov, Appl. Phys. Lett. **88**, 212503 (2006).
[13] G. Hampel, B. Batlogg, K. Krishana, N. P. Ong, W. Prusseit, H. Kinder, and A. C. Anderson, Appl. Phys. Lett. **71**, 3904 (1997).
[14] J. Halbritter, J. Supercond. **8**, 691 (1995).
[15] T. L. Hylton, A. Kapitulnik, M. R. Beasley, J. P. Carini, L. Drabeck, and G. Grüner, Appl. Phys. Lett. **53**, 1343 (1988).
[16] A. V. Velichko, M. J. Lancaster, and A. Porch, Supercond. Sci. Technol. **18**, R24 (2005).
[17] A. Yu. Aladyshkin, A. A. Andronov, E. E. Pestov, Yu. N. Nozdrin, V. V. Kurin, A. M. Cucolo, R. Monaco, and M. Boffa, Radiophys. Quantum Electron. **46**, 109 (2003).
[18] P. N. Micheenko and Yu. E. Kuzovlev, Physica C **204**, 229 (1993).
[19] A. V. Bobyl, M. E. Gaevskii, S. F. Karmanenko, R. N. Kutt, and R. A. Suris, J. Appl. Phys. **82**, 1274 (1997).
[20] R. Wordenweber, Supercond. Sci. Technol. **12**, R86 (1999).
[21] A. De Luca, A. F. Degardin, F. Abbott, F. Houze, and A. J. Kreisler, Physica C **372-376**, 578 (2002).
[22] E. E. Pestov, V. V. Kurin, and Yu. N. Nozdrin, IEEE Trans. Appl. Supercond. **11**, 131 (2001).

[23] J. R. Clem and R. P. Huebener, J. Appl. Phys. **51**, 2764 (1980).
[24] M. E. Gaevski, A. V. Bobyl, S. G. Konnikov, D. V. Shantsev, V. A. Solov'ev, and R. A. Suris, Scanning Microsc. **10**, 679 (1996).
[25] D. V. Shantsev, M. E. Gaevski, R. A. Suris, A. V. Bobyl, V. E. Gasumyants, and O. L. Shalaev, Phys. Rev. B **60**, 12485 (1999).
[26] X. C. Zeng, D. J. Bergman, P. M. Hui, and D. Stroud, Phys. Rev. B **38**, 10970 (1988).
[27] K. K. Likharev, *Dynamics of Josephson Junctions and Circuits* (Gordon and Breach, New York, 1986).
[28] B. L. van der Waerden, *Mathematical Statistics* (Springer-Verlag, Berlin, 1969).
[29] D. Seron, D. E. Oates, G. Hammerl, J. Mannhart, P. J. Hirst, R. G. Humphreys, A. C. Anderson, M. A. Hein, and J. Derov, Phys. Rev. B **72**, 104511 (2005).
[30] B. A. Willemsen, K. E. Kihlstrom, T. Dahm, D. J. Scalapino, B. Gowe, D. A. Bonn, and W. N. Hardy, Phys. Rev. B **58**, 6650 (1998).
[31] T. S. Argunova, R. N. Kyutt, M. P. Scheglov, and N. N. Faleev, J. Phys. D **28**, A212 (1995); A. G. Zaitsev, P. Wordenweber, T. Koning, E. K. Hollman, S. V. Rasumov, and O. G. Vendik, Physica C **264**, 125 (1996).